

# IMPROVING THE HEAT TRANSFER CHARACTERISTICS OF THE SPIKY CENTRAL RECEIVER AIR PRE-HEATER (SCRAP) USING HELICALLY SWIRLED FINS

Dewald Grobbelaar<sup>1</sup>, Matti Lubkoll<sup>2</sup>, Theodor W von Backström<sup>3</sup>

<sup>1</sup> Solar Thermal Energy Research Group (STERG), Department of Mechanical and Mechatronic Engineering, Stellenbosch

University, South Africa; 17157668@sun.ac.za

<sup>2</sup> Stellenbosch University; matti@sun.ac.za

<sup>3</sup> Stellenbosch University; twvb@sun.ac.za

## Abstract

A combined cycle concentrating a solar power (CSP) system, such as the Stellenbosch University Solar Power Thermodynamic (SUNSPOT) cycle requires a novel receiver technology capable of heating pressurized air. The Spiky Central Receiver Air Pre-heater (SCRAP) receiver technology was conceived with the aim of providing a robust, metallic receiver technology, capable of heating air at high efficiency to elevated temperatures. The SCRAP receiver uses an internal extended surface in the absorber assemblies (spikes) to increase the heat transfer performance. In the current configuration, straight trapezoidal fins form rectangular passages through which the air stream passes and heated to approximately 800 °C.

The use of helically swirled fins within the SCRAP model is intended to improve the heat transfer characteristics by increasing the effective surface, by increasing the heat transfer coefficient and by introducing a balancing effect around the circumference of a spike, as it may not experience homogenous irradiation.

**Key words:** CSP, central receiver, SCRAP, helically swirled fins, heat transfer improvement.

## 1. Introduction

Solar power is a source of energy with immense potential. A system such as a (CSP) plant is one of the ways to harness solar energy. This rapidly evolving technology contributes to the renewable and sustainable energy agenda of the world.

One of the ways to enhance efficiency is the combined cycle, using a topping Brayton cycle and a bottoming Rankine cycle. A manifestation of such a cycle is the SUNSPOT cycle [1].

Stellenbosch university is currently investigating this SUNSPOT cycle. This specific system, shown in figure 1, differs from other systems by using air instead of oil as working fluid in a combined cycle.

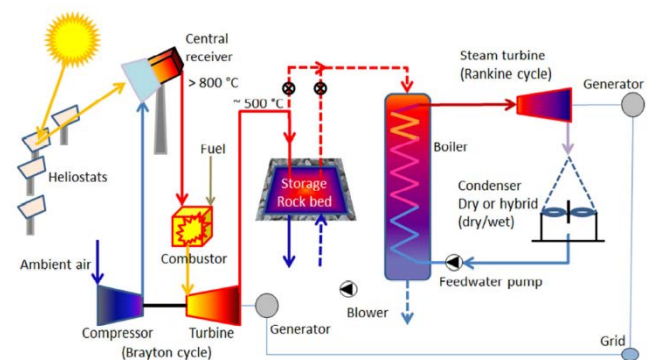


Figure 1: SUNSPOT cycle [1]

Due to this difference, new air receiver technologies have to be investigated to heat the air temperature before it is utilised by gas turbine. This is where the SCRAP (spiky central receiver air pre-heater) receiver concept was introduced. Lubkoll [1] indicates a potential design for the spikes in the receiver.

The purpose of this paper is to establish to what extent the heat transfer characteristics can be improved while considering the increase in pressure drop in the system by adapting the current design.

The initial analysis suggested an increase in heat transfer characteristics with moderate pressure losses. The CFD analysis was done and provided motivation for experimental testing.

The main goal of a concentrating solar plant (CSP) is to effectively absorb radiation reflected to the plant's receiver

whilst keeping losses, which include radiation losses, reflection losses and convective losses, to a minimum. With the SCRAP receiver concept, the radiation losses are minimised due to the view factors back to the external environment to the receiver being very small. The tip of a spike has a large view factor, but it is constantly being impinged with cold air making the heat transfer efficiency very high. The volumetric effect can also somewhat be achieved within the spikes [1].

Further improvement on the receiver can be done by improving the heat transfer characteristics of the spikes. By improving the rate at which the working fluid (air) absorbs heat from the metal spikes, the possibility for heat to be lost to the surroundings can be minimized. Taking this into account shows that improving the spikes are of vital importance.

To date not many pressurized air receivers have been considered because volumetric cavity receivers can reach much higher temperatures [2]. Even though the SCRAP system cannot reach these elevated temperature, the system has been proven to be more robust, cheaper and less complex [2]. The SCRAP is an external tubular receiver with a multitude spikes surrounding the receiver centre. The spikes are concentrically arranged with increasing density toward the centre of the receiver as shown in figure 2.

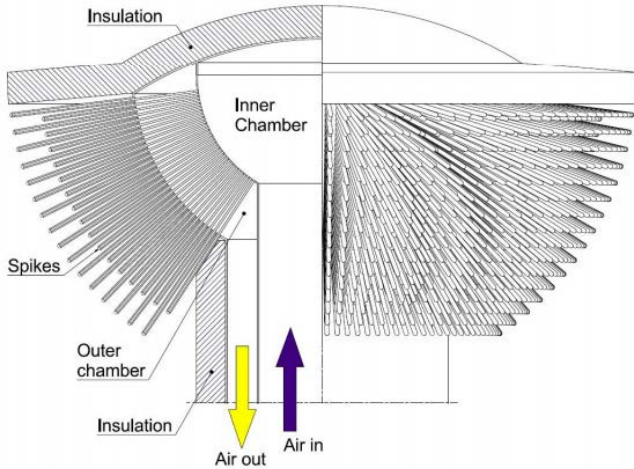


**Figure 2: SCRAP receiver with cross-section [1]**

Cold air enters in the centre of the receiver, from there the air enters the spikes. The spikes consist of two concentric tubes, an inner and outer tube. The cold air travels through the inner tube towards the tip of the spike. The cold air hits the spike tip at which stage it is redirected back 180° and travels along the outer tube as seen in figure 3. Concentrated rays heat up the tip and

outer area of the spike, heat is transferred through the spike to the air.

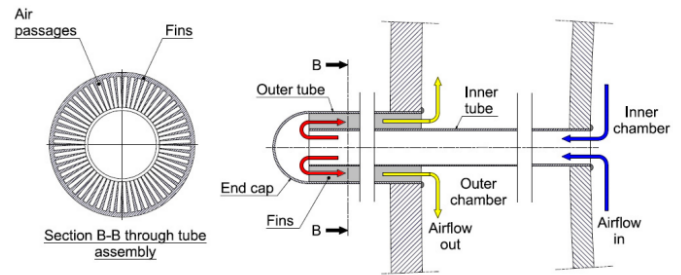


**Figure 3: Straight tube geometry [1]**

The air returns through rectangular tubes within the outer tube. These rectangular tubes improve the heat transfer characteristics, thus transferring the heat much quicker to the heat transfer fluid, namely air. The air then returns to an outer chamber from where it exits the receiver.

### 1.1 Objectives

The main objective of the project is to investigate the effect of helically swirled fins on the design and test a SCRAP spike section to improve the heat transfer characteristics/efficiency. The objectives are the following:

1. Determine the angle at which the helically swirled fins would clearly show increase in heat transfer.
2. Investigate the effect of the fins on the pressure drop.
3. Design the spiky central receiver air pre-heater with helically swirled fins.
4. Model the spiky central receiver air pre-heater's helically swirled fins with the use of CFD.

## 2. Comparison of empirical correlations

Several approaches were used to calculate the theoretical values of the Nusselt numbers and friction factors in helically swirled ducts. These results are compared to that of a straight rectangular duct calculated by using the VDI heat atlas [3].

### 2.1 Straight duct

For comparison calculations on a straight duct was conducted. The friction factors and Nusselt numbers are calculated using the following equations [3]:

$$f_s = 0.3164Re^{-0.25} \quad (1)$$

and

$$Nu_s = 0.021 \times Pr^{0.5} \times Re^{0.8} \quad (2)$$

where  $f_s$  is the friction factor of a straight duct,  $Nu_s$  is the Nusselt number of a straight duct,  $Pr$  is the Prandtl number and  $Re$  is the Reynolds number.

## 2.2 VDI

All the VDI correlations are founded by applying a constant heat flux. Standard geometry of a coil [3] is given by Figure 4.

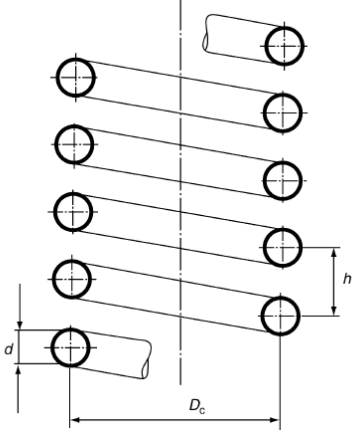


**Figure 4: Coil geometry**

$D_c$  is the coil diameter,  $d$  the tube diameter and  $h$  is the pitch of the coil. Using the hydraulic diameter, the equations in VDI can be applied to a rectangular duct. It is stated that  $Nu$  stays within a 15% error when using the following equations [3]:

$$Nu = 3.66 + 0.08 \left[ 1 + 0.8 \left( \frac{d}{D_c} \right)^{0.9} \right] Re^m Pr^{\frac{1}{3}} \left( \frac{Pr}{Pr_w} \right)^{0.14} \quad (3)$$

valid for laminar flow ( $Re \leq Re_{crit}$ ), where  $Pr_w$  is the Prandtl number at the wall,

$$m = 0.5 + 0.2903 \left( \frac{d}{D_c} \right)^{0.194} \quad (4)$$

and

$$Re_{crit} = 2300 \left[ 1 + 8.6 \left( \frac{d}{D_c} \right)^{0.45} \right] \quad (5)$$

For turbulent flow,  $Re > 2.2 \times 10^4$ , the following equations are applied:

$$Nu = \frac{\left( \frac{\zeta}{8} \right) Re Pr}{1 + 12.7 \sqrt{\frac{\zeta}{8}} \left( Pr^{\frac{2}{3}} - 1 \right)} \left( \frac{Pr}{Pr_w} \right)^{0.14} \quad (6)$$

where

$$\zeta = \left[ \frac{0.3164}{Re^{0.25}} + 0.03 \left( \frac{d}{D_c} \right)^{0.5} \right] \left( \frac{\eta_w}{\eta} \right)^{0.27} \quad (7)$$

and  $\eta_w$  and  $\eta$  is the dynamic viscosity of the fluid at the wall and the fluid standard dynamic viscosity respectfully

## 2.3 Kakac

Kakac's correlations are described based on boundary conditions of uniform wall temperature and uniform wall heat flow. According to Kakac et al [4] the measured Nusselt number at the outer wall of a helical coil is about 1.5 times that of a straight tube and on the inner wall is about 0.5 that of a straight tube. This means that the overall Nusselt number of a helical coil is 20-30% higher than a straight tube [4]. This is also true for the concept of hydraulic diameter which applies for rectangular swirled tube.

The equation provided to calculate Nusselt number for multiple Reynolds numbers is as follow:

$$\frac{Nu_c}{Nu_s} = 1.0 + 3.6 \times \left[ 1 - \left( \frac{a}{R} \right) \right] \left( \frac{a}{R} \right)^{0.8} \quad (8)$$

where  $Nu_c$  is the Nusselt number for a coil,  $a$  the major axis of an ellipse or rectangle and  $R$  the coil radius which is valid for  $20\,000 < Re < 150\,000$  and  $5 < R/a < 84$

For lower Reynolds numbers, the following equation is used:

$$\frac{Nu_c}{Nu_s} = 1.0 + 3.4 \left( \frac{a}{R} \right) \quad (10)$$

This equation is valid for  $1500 < Re < 20\,000$ .

where

$$Nu_s = 0.021 \times Pr^{0.5} \times Re^{0.8} \quad (11)$$

For the range of  $1500 < Re < 8000$  the friction factor is calculated using the following equation:

$$\frac{f_c}{f_s} = 0.435 \times 10^{-3} Re^{*0.93} \left( \frac{R}{d^*} \right)^{0.22} \quad (12)$$

where

$$f_s = 0.3164 Re^{-0.25}, \quad (13)$$

$$Re^* = Re \times \frac{\text{width of rectangle}}{\text{hydraulic diameter}} \quad (14)$$

and  $d^*$  is the width of the rectangular duct

Then for  $Re > 8000$

$$f_c \left(\frac{R}{a}\right)^{0.5} = 0.084 \left[ Re \left(\frac{R}{a}\right)^{-2} \right]^{-0.2} \quad (15)$$

These equations are in good correlation with experimental data for air and water and stay within a 10 % variation [4]. The friction factor is, the same as for Nusselt number, 1.5 times at the outer wall of the coil and 0.5 times at the inner wall of the coil [4].

The last two equations used to calculate the Nusselt numbers are the Kaya and Teke [5] and the Xin and Ebadian [6] methods.

#### 2.4 Kaya and Teke [5]:

$$Nu = 0.023Re^{0.8}Pr^{0.4} \left[ 1.0572 + 0.1761 \left(\frac{d}{D_c}\right) \right] \quad (16)$$

#### 2.5 Xin and Ebadian [6]:

$$Nu = 0.00619Re^{0.92}Pr^{0.4} \left( 1 + 3.455 \left(\frac{d}{D_c}\right) \right) \quad (17)$$

The results obtained for all the calculations of Nusselt number and friction factor are shown in Figures 5 and 6.

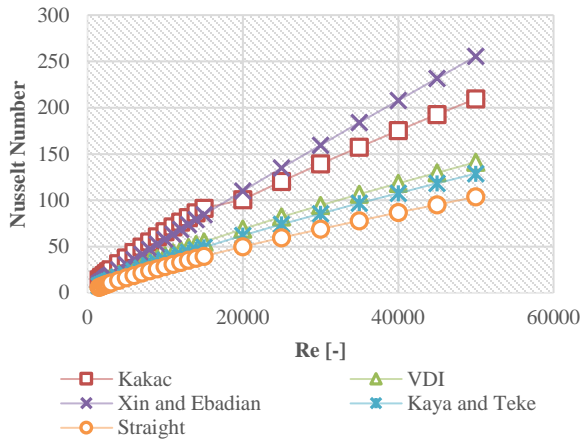


**Figure 5: Nusselt number vs Reynolds number**

The results of the different methods of calculating the Nusselt number and friction factor of helically swirled ducts are all an improvement from the straight duct even though they differ from each other due to the assumptions made to correlate the equations.

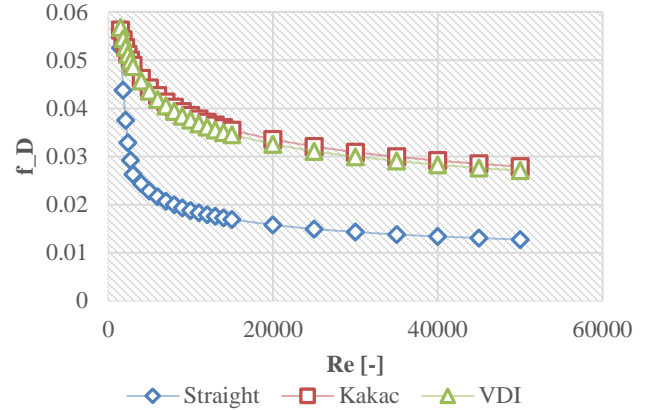


**Figure 6: Friction factor vs Reynolds number**

The pressure drop is calculated using the friction factor obtained in each of the methods and the following equation [7]:

$$\Delta p = \left(\frac{L}{D_h}\right) \frac{\rho V^2}{2} \quad (18)$$

where  $\Delta p$  is the pressure drop,  $L$  is the length of the tube,  $D_h$  is the hydraulic diameter,  $\rho$  is the density of the working fluid and  $V$  is the velocity. Figure 7 shows the pressure drop predicted for each of the calculated methods.

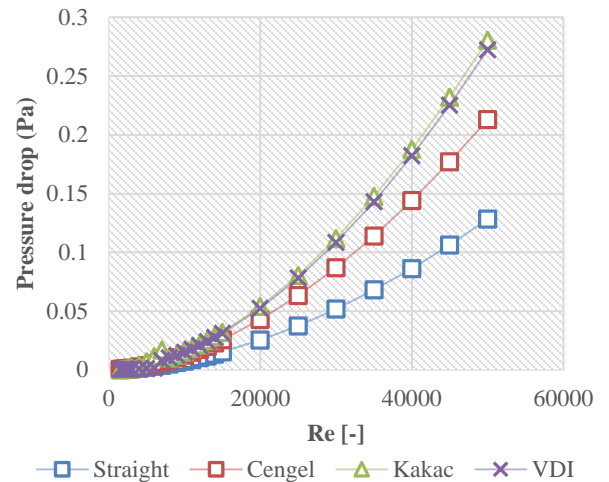


**Figure 7: Pressure drop vs Reynolds number**

Considering Figures 5 and 7, it is shown that the increase in heat transfer capabilities comes at the cost of an increased pressure drop. The pressure loss can be overcome by increasing the discharge head in the system.

In conclusion, the correlations provide motivation to further investigate the effect helically swirled ducts could have on the heat transfer in a SCRAP system.

### 3. Numerical Simulation

The calculations provided motivation to model a simulation for further investigation on the effect helically swirled fins will have on the heat transfer rate. The numerical simulation was modelled in Ansys FLUENT.

#### 3.1. Geometry

The geometry of the CFD simulation was modelled to be comparable to a present experimental setup located at Stellenbosch university. This will make the future validation of the experiment easier.

The SCRAP test part consists of 24 symmetrical fins. Thus, only one fin with symmetry conditions had to be modelled. The length of the simulated fins is 200mm, with one full rotation present and is shown in more detail in figure 8. The inner gap is the flow area whereas the solid outer part is the fin section.

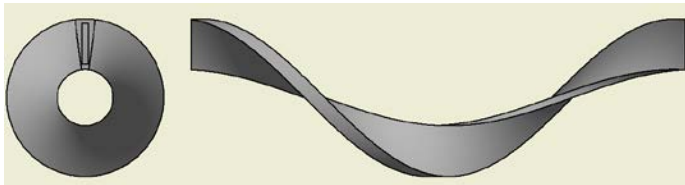


Figure 8: Computational geometry

#### 3.2. Mesh

The mesh was designed to have a considerable number of cells in the fluid domain to see any effects of secondary flows.

A very coarse mesh is present in the solid part due to no actual information being needed from it, but it serves as the heat transfer material, transferring the heat from the outer hot surface to the inner working fluid. Figure 9 shows partially the first detailed mesh of the fluid domain and coarse mesh of the solid domain.

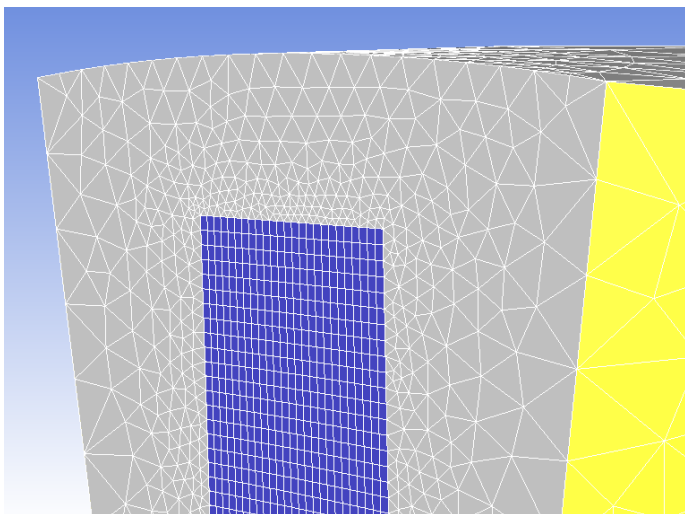


Figure 9: Mesh

The mesh was then refined to reduce the y-plus value, but it did not suffice. A new tetra mesh was then implemented and refined. The final redefined mesh is shown in Figure 10.

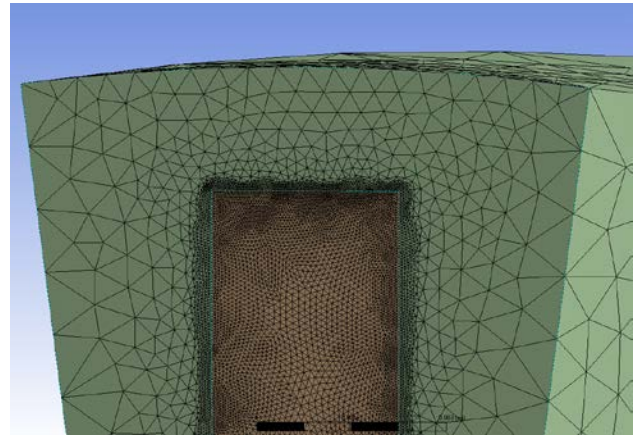


Figure 10: Redefined mesh

#### 3.3 General settings

The k-epsilon realizable model was implemented. The reason for this model is because this model contains the new formulation for the turbulent viscosity and a new transport equation for dissipation rate. This model is mathematically more correct and consistent with physics of turbulent flow than the standard k-ε turbulent model. The calculation of gradient terms was set as least square cell based. The pressure discretization was set to second order and finally all the other discretization terms were set to second order upwind.

#### 3.4 Results

The results obtained show secondary flow occurring within the fin. Secondary flow occurs in and around the higher-pressure areas within a duct. Figure 11 shows the high pressure area in the top left corner.

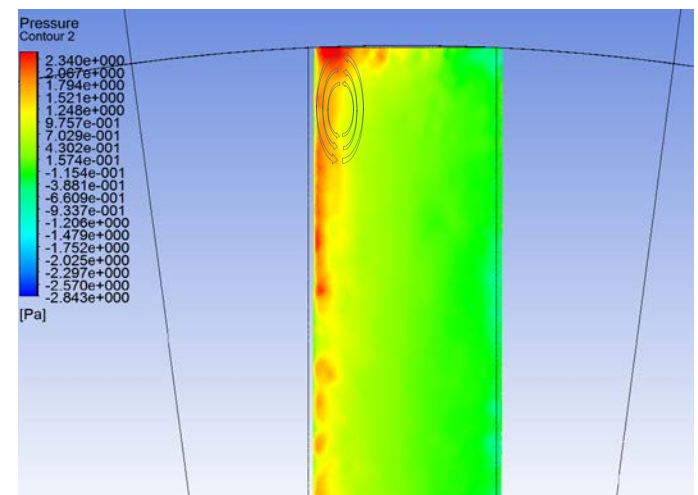


Figure 11: Pressure profile at outlet

The velocity magnitude field in cross section is shown in Figure 12 and is greatest in the bottom left corner and reduces towards the top right corner. This image shows the velocity magnitude which includes the velocity down the tube length.

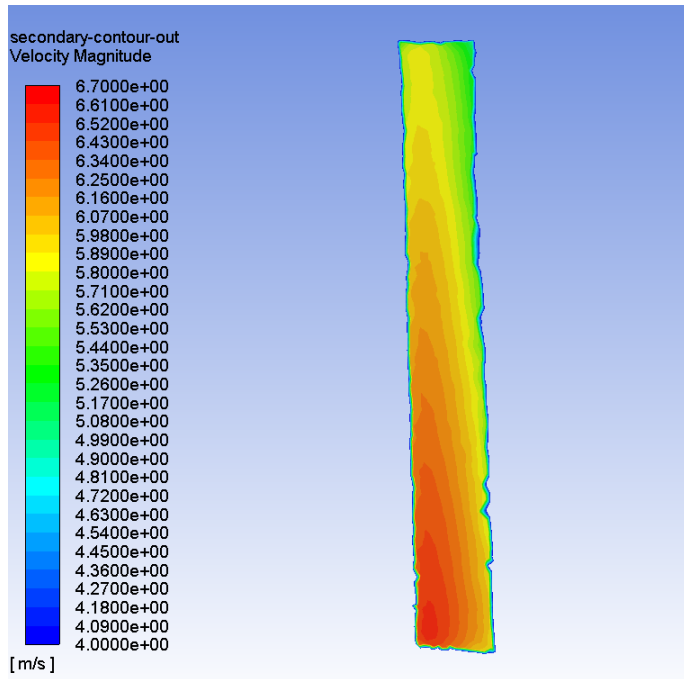


Figure 12: Velocity magnitude profile at outlet

Figure 13 shows the velocity field in cross section along the axial direction thus excluding the velocity down the tube length and visible showing secondary flow contours.

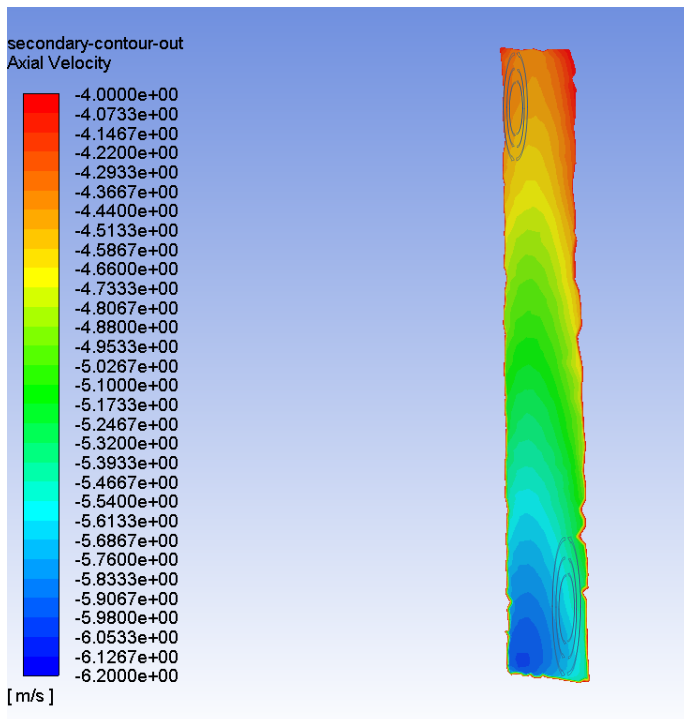


Figure 13: Axial velocity profile at outlet

The axial velocity is smallest in the bottom left corner and increases towards the top right. The contour show that vertices form with their centres being at the top left and bottom right corners, spreading out from there [8].

An increase in Nusselt number is present in further down the flow domain shown in Figure 14. A further increase would be possible with more than one rotational turn but due to comparison reasons it is kept at one rotation.

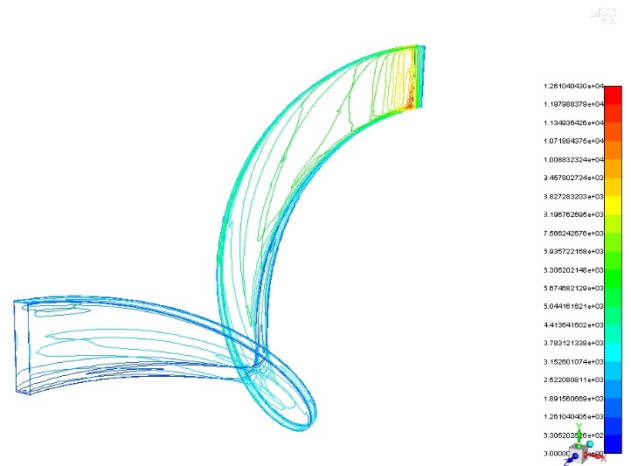


Figure 14: Nusselt number along fluid domain

The simulation provides the necessary motivation for experimental testing and can be used for future comparison and validation of the experimental work.

#### 4. Prototype design

The prototype is designed to be compatible with a test setup located at Stellenbosch university. The test part will be manufactured using advanced additive manufacturing due to the challenging geometry the helical fins possess.

##### 4.1. CAD design

The design is made so the fins turn one full rotation within the testing length of 200mm. This is done to ensure that the effect of secondary flow is present in the system. The final design is shown in figure 15.

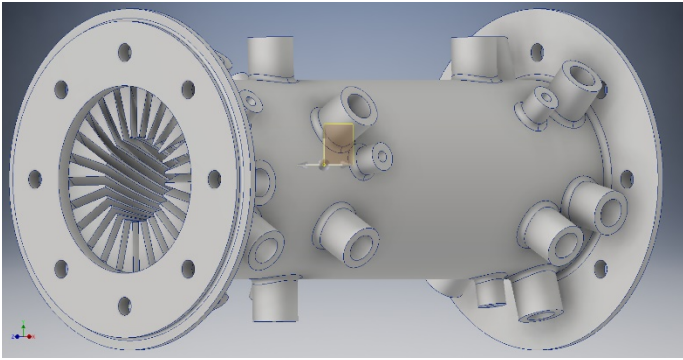


**Figure 15: Helically finned test part**

There are several fittings on the test part; the purpose of these are for the thermocouples and pressure taps to attach to the test part for measurements. Three different ducts have three pressure taps along the length of the tube, two of the pressure taps are close to the duct entrance and one towards the end, this is done because the numerical simulation showed the flow develops quickly.

There is a total of 24 thermocouple fitting. Three locations, one close to the entrance, one 88mm from the entrance and one close to the end each had six thermocouples fitted with different measuring depths in the fins. Two other locations have three thermocouple fittings with the same measuring depth in each fin.

## 5. Conclusion

The initial analysis suggested an increase in heat transfer characteristics with surmountable pressure losses. The numerical simulation supports the initial analysis in showing high heat transfer rates due to secondary flows.

Nusselt numbers in the simulation correlate with the calculations in showing improvement because of the rotation. The numerical simulation analysis provides motivation to pursue the possibility of experimental testing and can also be used to validate experimental test results.

This research shows how the SCRAP design shows potential and can be even further improved. With further research on the material properties to improve the tube material heat transfer characteristics, the SCRAP model can contribute to making combined cycle CSP plants feasible.

## Acknowledgements

I would like to express my sincere gratitude to the following people:

- The Centre for Renewable and Sustainable Energy Studies (CRSES) at Stellenbosch University for funding to attend the conference.

## References

- [1] Lubkoll M. (2017), *Performance Characteristics of a Spikey Central Receiver Air Pre-heater (SCRAP)*, Thesis, (PhD), Stellenbosch university, Stellenbosch.
- [2] Kröger, D. G. (2008), *Spikey Central Receiver Air Pre-heater (SCRAP)*, Technical report, Stellenbosch university, Stellenbosch.
- [3] VDI e.V. 10<sup>th</sup> edition (2010), *VDI Heat Atlas*, New York: Springer.
- [4] Kakac S. Ramesh K. Shah, Win Aung. (1987), *Handbook of single-phase convective heat transfer*, New York: Wiley.
- [5] Kaya O. Teke I. (2005), Turbulent forced convection in a helically coiled square duct with one uniform temperature and three adiabatic walls, *Heat and Mass Transfer*, Vol.42(2), pp. 129-137.
- [6] Xin R. C. Ebadian M.A. 1997, 'The effects of Prandtl numbers on local and average convective heat transfer characteristics in helical pipes', *J. Heat report, Transfer*, vol 119, no 3, pp 467-473
- [7] White, F. (1991). *Viscous Fluid Flow*. 2nd edn. McGraw-Hill, Inc., New York. ISBN 0-07-069712-4.
- [8] Xing Y. Zhong F. Zhang X. 2014, 'Numerical Study of Turbulent Flow and Convective Heat Transfer Characteristics in Helical Rectangular Ducts', *J. Heat Transfer*, vol 136,